10 December 1999

ELSEVIER

Chemical Physics Letters 314 (1999) 488–495

CHEMICAL PHYSICS LETTERS

www.elsevier.nl/locate/cplett

Two-dimensional line-shape analysis of photon-echo signal

Ko Okumura *, Andrei Tokmakoff [a], Yoshitaka Tanimura

Division of Theoretical Studies, Institute for Molecular Science, Myodaiji, Okazaki, Aichi 444-8585, Japan
[a] *Department of Chemistry, Massachusetts Institute of Technology, Cambridge, MA 02139, USA*

Received 2 August 1999; in final form 22 September 1999

Abstract

We analyze the two-dimensional (2D) line shape obtained by 2D Fourier transforming the time-domain response of a photon-echo signal as a function of the two coherence periods, t_1 and t_3. The line shape obtained for a two-level system with homogeneous and inhomogeneous broadening is shown to be sensitive to the magnitude of both of these line-broadening mechanisms. It is shown that the ellipticity of the 2D line shape can be related to the ratio of homogeneous to inhomogeneous broadening. © 1999 Elsevier Science B.V. All rights reserved.

The molecular spectrum in the condensed phase is usually broad and featureless from a convolution of all the dynamical and static information within it. Accordingly, much of the efforts of researchers have been paid to how one can extract information on the broadening mechanisms from these peaks. In the simplest sense, the broadening arises from two different aspects of the solvent. One is the dynamical evolution induced by the fluctuation of the solvent molecules, i.e., by the solvent–solute interaction. Another is the distribution of local environments about each molecule. Historically, the former has been referred as homogeneous or fast modulation, and the latter as inhomogeneous or the static contribution. The separation of these contributions from a conventional line-shape analysis fails because the signal is a convolution of these line-broadening mechanisms [1]. It is generally the case for one-dimensional (1D) observables – those that have one independent time or frequency variable – that one cannot uniquely extract information on multiple superimposed dynamical time scales.

One of the most effective tools at distinguishing multiple time scales in the dynamics of liquids is the photon-echo experiment [1]. Various approaches to this rephasing experiment have been applied to extracting the dynamic and static contributions to electronic and vibrational line shapes. In the classic integrated two-pulse photon echo, an initially created coherence is rephased by a time-delayed rephasing pulse, and the time-integrated amplitude of the field radiated from the induced polarization is measured. This experiment is particularly selective to the microscopic dynamics for a system with a clear separation of time scales, i.e. homogeneous dynamics masked by inhomogeneous broadening. Thus, these types of methods have been most successful in the study of low-temperature electronic dephasing in glasses [2] and the vibrational dynamics in liquids [3]. Electronic dephasing in liquids shows no such

* Corresponding author: Fax: +81-564-53-4660; e-mail: okumura@ims.ac.jp

0009-2614/99/$ - see front matter © 1999 Elsevier Science B.V. All rights reserved.
PII: S0009-2614(99)01173-2

separation of time scales, a limit under which the integrated echo becomes ambiguous [1,4]. Other versions of this experiment have been used to accommodate these problems. The three-pulse photon echo [2,5] and three-pulse photon-echo peak shift [6,7] have been used to extract a spectral density (or distribution function) for spectral diffusion dynamics. The fundamental goal of extracting the dynamics of the ensemble is present in this experiment, if the time evolution of the polarization induced by the final interaction field can be observed rather than the integrated intensity. This has been the motivation for the gated photon echo [8] and the heterodyne-detected stimulated photon echo [9]. (The Raman echo [10] is in essence a gated photon echo.) These two experiments are remarkably powerful by virtue of being two-dimensional (2D); they measure the magnitude of a non-linear polarization as a function of the two independent coherence evolution periods. The gated photon echo is proportional to the modulus squared of the third-order response function while the heterodyne-detected stimulated photon echo is a phase-sensitive measure of that quantity. (Functionally, the methods of spectral interferometry in the detection of the echo are equivalent [11].) The 2D nature of these experiments is only beginning to be exploited [12]. In this Letter, we aim to demonstrate that the line shape obtained from the spectral representation of a gated photon echo provides a clear qualitative picture and quantitative description of the static and dynamic contribution to a condensed-phase line shape. We will show that 2D Fourier transformed data enables us to obtain the dephasing times of both homogeneous and inhomogeneous broadening at the same time. We refer this type of analysis 2D line-shape (2DLS) analysis contrasting it with the conventional linear line-shape analysis.

In the following, we briefly review the theoretical background [1] of the photon echo. There are two reasons for this; one is to specify our notation while the other is to clarify some points which have not been properly or coherently discussed in the literature.

We describe the two lowest electronic levels by the Hamiltonian

$$H_0 = |g\rangle\langle g|H_g + |e\rangle\langle e|\left(H_e + \hbar\omega_{eg}\right), \tag{1}$$

where $\hbar\omega_{eg}$ is the electronic transition energy. The nuclear dynamics is described by the two nuclear coordinates and their conjugate momenta $(P_{\mathrm{H}},Q_{\mathrm{H}})$ and $(P_{\mathrm{I}},Q_{\mathrm{I}})$. These degrees of freedom are coupled to the heat bath and correspond to the homogeneous and inhomogeneous dynamics, respectively. The nuclear Hamiltonian H_g and H_e are given by $(\alpha = g,e)$

$$H_\alpha = \sum_{\mathrm{s}=\mathrm{H,I}} \left(\frac{P_{\mathrm{s}}^2}{2M_{\mathrm{s}}} + V_\alpha^{(\mathrm{s})}(Q_{\mathrm{s}}) + \sum_j \left\{ \frac{\left(p_j^{(\mathrm{s})}\right)^2}{2m_j^{(\mathrm{s})}} + \frac{m_j^{(\mathrm{s})}\left(\omega_j^{(\mathrm{s})}\right)^2}{2} \left[q_j^{(\mathrm{s})} - \frac{c_j^{(\mathrm{s})}Q_{\mathrm{s}}}{m_j^{(\mathrm{s})}\left(\omega_j^{(\mathrm{s})}\right)^2} \right]^2 \right\} \right). \tag{2}$$

In this model, the two modes $(Q_{\mathrm{I}},Q_{\mathrm{H}})$ are independent. Note that different sets of bath oscillators are introduced for each primary mode Q_{s}, while only one set is introduced in Eq. (8.61b) of Ref. [1]. It is our Hamiltonian that leads to the simple and physical classical equation of motion

$$M_{\mathrm{s}}\frac{\mathrm{d}^2Q_{\mathrm{s}}(t)}{\mathrm{d}t^2} + \frac{\mathrm{d}V_\alpha^{(\mathrm{s})}(Q_{\mathrm{s}})}{\mathrm{d}Q_{\mathrm{s}}(t)} + M_{\mathrm{s}}\int_0^t \mathrm{d}t'\,\gamma_{\mathrm{s}}(t-t')\frac{\mathrm{d}Q_{\mathrm{s}}(t')}{\mathrm{d}t'} = R_{\mathrm{s}}(t)\,. \tag{3}$$

The friction kernel $\gamma_{\mathrm{s}}(t)$ and the fluctuating force $R_{\mathrm{s}}(t)$ are a function of the bath parameters $(c_j^{(\mathrm{s})},m_j^{(\mathrm{s})},\omega_j^{(\mathrm{s})})$, and satisfy the relations, $\langle R_{\mathrm{s}}(t)\rangle = 0$ and $\langle R_{\mathrm{s}}(t)R_{\mathrm{s}'}(t')\rangle = \delta_{\mathrm{ss}'}2M_{\mathrm{s}}\gamma_{\mathrm{s}}(t-t')/\beta$. Here, $\delta_{\mathrm{ss}'}$ and $1/\beta$ are the Kronecker delta and the temperature (multiplied by the Boltzmann constant), respectively. When $\alpha = g$ (or $\alpha = e$) in the above Langevin equation of motion, it corresponds to the nuclear dynamics in the electronic ground (or first-excited) state.

In the above, we have assumed the two modes Q_{I} and Q_{H} do not interact with each other and that the random forces associated with them are also independent. These assumptions should be acceptable at least at the first level of approximation, considering that the two modes represent the two limiting cases, i.e., homogeneous and inhomogeneous (see below).

The two state $|g\rangle$ and $|e\rangle$ are independent except for the dipole interaction with the external electric field

$$H_{\mathrm{I}} = E(\boldsymbol{r},t)V, \tag{4}$$

where

$$V = \mu(Q_{\mathrm{H}},Q_{\mathrm{I}})(|g\rangle\langle e| + |e\rangle\langle g|). \tag{5}$$

The system is then described by the total Hamiltonian

$$H = H_0 + H_{\mathrm{I}}.$$

This two-level system is initially in the thermal equilibrium in the electronic ground state, which is characterized by the density matrix,

$$\rho_{\mathrm{I}} = \mathrm{e}^{-\beta H_g}|g\rangle\langle g|/\mathrm{Tr}[\mathrm{e}^{-\beta H_g}]. \tag{6}$$

In the photon-echo experiment, we apply the electric field (see Fig. 1), $E(\boldsymbol{r},t) = \sum_{i=1}^{3} E_i(\boldsymbol{r},t)$, where $E_i(\boldsymbol{r},t) = E_i(t)(\mathrm{e}^{i\boldsymbol{k}_i\cdot\boldsymbol{r}-i\omega_i t} + \mathrm{c.c.})$. Here, the envelopes are given as $E_i(t) = E_0\,\delta_{\mathrm{phys}}(t-t_i)$, where $t_1 = t_m - T_3 - T_2 - T_1$, $t_2 = t_m - T_3 - T_2$, $t_3 = t_m - T_3$. Here, t_m is the time of measurement of the signal while $\delta_{\mathrm{phys}}(t)$ implies a Gaussian-type function whose width is larger than optical cycle $(1/\omega_i)$ but much smaller than the nuclear time scale. We assume that these three pulses are well separated compared with the width of $\delta_{\mathrm{phys}}(t)$; T_1, T_2, T_3 are positive and larger than the width. Throughout this Letter, T_1, T_2, and T_3 always represent the first, second, and third delay times, respectively.

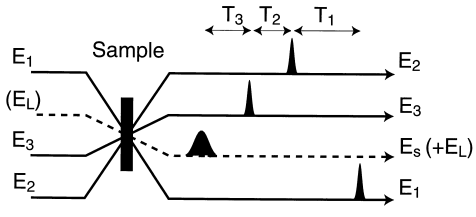

Fig. 1. The pulse configuration of the photon-echo experiment. By the first pulse E_1, the system is brought in the electronic coherence state, which is characterized by $|g\rangle\langle e|$ and $|e\rangle\langle g|$. The second pulse brings the system back to a population state $|g\rangle\langle g|$ or $|e\rangle\langle e|$. The third pulse makes the system again in the coherence state. Thus, the first and last delay times correspond to the coherence dephasing times, while the second to the population relaxation. E_{L} stands for the local oscillator field used in the heterodyne detection.

The photon echo is generated through the third-order process in terms of electric field. The relevant macroscopic polarizability is formally given as

$$P^{(3)}(\boldsymbol{r},t) = \int_{-\infty}^{\infty}\mathrm{d}t_3\int_{-\infty}^{\infty}\mathrm{d}t_2\int_{-\infty}^{\infty}\mathrm{d}t_1\,R^{(3)}(t_3,t_2,t_1) \times E(\boldsymbol{r},t-t_3)\,E(\boldsymbol{r},t-t_3-t_2) \times E(\boldsymbol{r},t-t_3-t_2-t_1), \tag{7}$$

where the third-order response function is given by

$$R^{(3)}(t_3,t_2,t_1) = \left(\frac{i}{\hbar}\right)^3\theta(t_1)\theta(t_2)\theta(t_3)\langle[[[V(t_1+t_2+t_3), V(t_1+t_2)],V(t_1)],V(0)]\rangle, \tag{8}$$

where, $\theta(t)$ is the step function. Here and hereafter, the average and the Heisenberg representation of operator are defined as $\langle X\rangle \equiv \mathrm{Tr}[\rho_{\mathrm{I}}X]/\mathrm{Tr}[\rho_{\mathrm{I}}]$ and $Y(t) \equiv \mathrm{e}^{iH_0t/\hbar}Y\mathrm{e}^{-iH_0t/\hbar}$.

The photon-echo measurement is a resonant experiment, which implies that ω_is are resonant with the electronic transition frequency ω_{eg}. Thus, we are allowed to use the rotating wave approximation (RWA). Furthermore, we introduce two approximations: the Condon approximation and the approximation of the second-order cumulant expansion. The former implies that we expand the dipole moment $\mu(Q_{\mathrm{H}},Q_{\mathrm{I}})$ in terms of the nuclear coordinates and keep only the first-order term, μ_0, which does not depend on nuclear coordinates. The latter is exact for harmonic (or Gaussian) nuclear dynamics as in the specific case considered below. Note that one can include anharmonicity of the potential perturbatively by using the generating functional approach [13].

Under these approximations, the macroscopic polarizability in the echo direction specified by $\boldsymbol{k}_{\mathrm{s}} = -\boldsymbol{k}_1 + \boldsymbol{k}_2 + \boldsymbol{k}_3$ is given by

$$P^{(3)}_{\boldsymbol{k}_{\mathrm{s}}}(\boldsymbol{r},t) = \mathrm{e}^{i\boldsymbol{k}_{\mathrm{s}}\cdot\boldsymbol{r}-i\omega_{\mathrm{s}}t}P^{(3)}_{\boldsymbol{k}_{\mathrm{s}}}, \tag{9}$$

where $\omega_{\mathrm{s}} = -\omega_1 + \omega_2 + \omega_3$, and

$$P^{(3)}_{\boldsymbol{k}_{\mathrm{s}}} = E_0^2E_0^*\,\mathrm{e}^{-i\omega_1T_1}\,\mathrm{e}^{i(\omega_2-\omega_1)T_2}\,\mathrm{e}^{i(\omega_3+\omega_2-\omega_1)T_3} \times R_{\mathrm{ech}}(T_3,T_2,T_1). \tag{10}$$

Here, we have employed the impulsive pulse limit where $\delta_{\rm phys}(t)$ can be treated as the Dirac delta function for the nuclear dynamics; as a result of the integration over time variables, the first, second, and third delay times (T_1, T_2, T_3) appear in the above expression.

The echo response function $R_{\rm ech}(t_3,t_2,t_1)$ is given by

$$R_{\rm ech}(t_3,t_2,t_1) = \mu_0^4(i/\hbar)^3\theta(t_1)\theta(t_2)\theta(t_3) \times e^{i\omega_{eg}(t_1-t_3)}[e^{f_1(t_1,t_2,t_3)} + e^{f_2(t_1,t_2,t_3)}], \quad (11)$$

where the auxiliary function has been introduced by

$$f_1(t_1,t_2,t_3) = -g(t_1)^* - g(t_1+t_2)^* + g(t_1+t_2+t_3)^* + g(t_2) - g(t_3)^* - g(t_2+t_3), \quad (12)$$

$$f_2(t_1,t_2,t_3) = -g(t_1)^* - g(t_1+t_2)^* + g(t_1+t_2+t_3)^* + g(t_2)^* - g(t_3) - g(t_2+t_3)^*, \quad (13)$$

where the line broadening function $g(t)$ is given as the correlation of fluctuation of the electronic transition energy:

$$g(t) = \int_0^t dt' \int_0^{t'} dt'' \langle U(t')U(t'')\rangle/\hbar^2, \quad (14)$$

where $U = H_e - H_g$. We employ a model with $\langle U\rangle = 0$ below (see Eqs. (15) and (16)), in which case U is the *fluctuation* around the transition energy $\hbar\omega$.

In general, $g(t)$ is essential for all linear or non-linear *resonant* optical measurements. This is because all kinds of signal can be calculated only if we know the form of $g(t)$ under the assumption of the second-order approximation of the cumulant expansion [1].

We assume that the adiabatic potentials for the nuclear coordinates in the ground and first excited states are both harmonic:

$$V_g^{(s)}(Q_s) = \frac{M_s\Omega_s^2}{2}Q_s^2, \quad (15)$$

$$V_e^{(s)}(Q_s) = \frac{M_s\Omega_s^2}{2}(Q_s+d_s)^2. \quad (16)$$

Thus, the line-broadening function $g(t)$ is given by the double time integration of $\langle Q_s(t)Q_s(0)\rangle$ in this case. We further assume that the damping constant in Eq. (3) is given by $\gamma_s(t) = \gamma_s\delta(t)$, where $\delta(t)$ is the Dirac delta function. This implies that we represent all the information of the bath parameters $(c_j^{(s)}, m_j^{(s)}, \omega_j^{(s)})$ by a single constant γ_s. In this Ohmic case, the correlation function $\langle Q_s(t)Q_s(0)\rangle$ is analytically given and, under the approximation (precisely specified below), the line-broadening function reduces to the Kubo's line-broadening function [14,1]

$$g(t) = \sum_{s=H,I} g_s(t), \quad (17)$$

where, for $t > 0$,

$$g_s(t) = \Delta_s^2\tau_s^2\left(e^{-t/\tau_s} + t/\tau_s - 1\right). \quad (18)$$

Here, Δ_s is the mean-square distribution of transition energies, i.e., $\Delta_s^2 = \langle U_s^2\rangle/\hbar^2$, where $U_s = V_e^{(s)}(Q_s) - V_g^{(s)}(Q_s)$ and $U = \sum_s U_s$, while τ_s is the correlation time of the transition energy fluctuations, i.e., $\tau_s = \int_0^\infty \langle U_s(t)U_s(0)\rangle\, dt/\Delta_s^2$. For $t < 0$, $g(t)$ is given by the same expression as the above one. Note here that $g(t)$ always satisfies the relation $g(-t) = g(t)^*$.

The approximations involved in the above are (1) that the nuclear dynamics for the two modes, Q_I and Q_H, are both overdamped ($\Omega_s \ll \gamma_s/2$) and (2) that the temperature satisfies the relation $1/\beta \gg \hbar\Omega_s(\Omega_s/\gamma_s)$. It should be noticed that this temperature condition is rather weak in this overdamped case ($\Omega_s/\gamma_s \ll 1$), although it is sometimes called *high temperature limit*.

As had been discussed by Kubo from the standpoint of the stochastic theory, the overall feature of the 1D line shape (1DLS) looks Gaussian for $\Delta_s\tau_s > 1$, while it looks Lorentzian for $\Delta_s\tau_s < 1$. The former has been called inhomogeneous while the latter homogeneous in the literature (but not by Kubo); we assume the relations $\Delta_I\tau_I > 1$ and $\Delta_H\tau_H < 1$. As suggested by Kubo, we can approximate $g_H(t)$ by its long-time approximation, while $g_I(t)$ by its short-time one:

$$g_H(t) = \Delta_H^2\tau_H t, \quad (19)$$

$$g_I(t) = \Delta_I^2 t^2/2. \quad (20)$$

The absorption spectrum corresponding to these line-broadening functions reduce to the homogeneous Lorentzian distribution with the width $\Gamma_H \equiv$

$\Delta_H^2 \tau_H$ and the inhomogeneous Gaussian distribution with the widths $\Gamma_I \equiv \Delta_I$, respectively.

We note here that, from the standpoint of the stochastic theory, the above two simple forms of the line-broadening function can be deduced not only from Eq. (18) but also from a quite general form. In this sense, these two simple forms can represent rather general features.

Although we have used the conventional words 'inhomogeneous' for g_I, dissipation by the Q_I mode results from the solute–solvent coupling or the homogeneous origin. The term 'inhomogeneous' is used to refer to the Gaussian shape. In the limit $\tau_I \to \infty$, the Q_I mode is actually inhomogeneous. However, we should note that, unless the ratio Δ_I/Δ_H is fixed, the relation $\tau_H < \tau_I$ does not *necessarily* hold in the present model; the inhomogeneous correlation time τ_I can be shorter than the homogeneous time τ_H if the inhomogeneous energy gap fluctuation Δ_I is larger than the homogeneous gap fluctuation Δ_H. In addition, *there is no restriction on the value* Γ_I/Γ_H *in general*. This might be the reason Kubo avoid using the word homogeneous or inhomogeneous.

If both the Lorentzian and Gaussian modes exist, the absorption spectrum takes on the form of a convolution of the Lorentzian and Gaussian contributions. The interpretation of the 1D line shape (1DLS) in this limit becomes ambiguous. As shown below, in the 2DLS analysis in which two variables are introduced, we can make a clear separation of these two components.

In this simple model, the echo response function $R_{ech}(t_3,t_2,t_1)$ reduces to

$$R(t_1,t_2) = 2\mu_0^4(i/\hbar)^3\theta(t_1)\theta(t_2)\theta(t_3) \times e^{i\omega_{eg}(t_1-t_3)}\, e^{-\Gamma_I^2(t_1-t_3)^2/2-\Gamma_H(t_1+t_3)}, \tag{21}$$

which is independent of T_2. In general, we can show that, if the real part of $g(t)$ is at most second order in t and if the imaginary part is at most first order in t, f_1 is independent of T_2, and, if $g(t)$ is at most the second order in t, $f_2(t)$ is independent of T_2. (This implies that the T_2 dependence of the signal is a clear indication of the deviation of the real system from this simple model. It is rather sensitive way of judging the applicability of this model.)

The signal $I_{HM}(T_1,T_2,T_3)$ obtained from the gated photon echo is proportional to $|P^{(3)}_{\boldsymbol{k}_s}(\boldsymbol{r},t)|^2 \sim |R_{ech}(T_3,T_2,T_1)|^2$, since the signal field $E_s(\boldsymbol{r},t)$ is proportional to the polarizability $P^{(3)}_{\boldsymbol{k}_s}$. Here and hereafter, $|X|$ denotes the absolute value of X. In our simple model, it reduces to $I_{HM}(T_1,T_2,T_3) \sim e^{-\Gamma_I^2(T_1-T_3)^2-2\Gamma_H(T_1+T_3)}$. In the conventional photon-echo experiment, we observe the integrated quantity $\int dT_3\, I_{HM}(T_1,T_2,T_3)$. If the Gaussian width Γ_I is large in the sense that the 'inhomogeneous' dephasing time is much smaller than the vibrational time scales, the factor $e^{-\Gamma_I^2(T_1-T_3)^2}$ can be treated as $\delta(T_1-T_3)$, and we have a purely homogeneous signal $I_{HM}(T_1,T_2,T_3) \sim e^{-4\Gamma_H T_1}$. By measuring the signal as the integrated one, we eliminate the 'inhomogeneity'. However, it is sometimes impossible to treat the factor as the delta function. In such a case, the elimination of the 'inhomogeneity' in the photon-echo experiment is incomplete [4].

The crucial quantity of this Letter is the 2D Fourier transformation of the echo response function

$$S_{2D}(\omega_3,T_2,\omega_1) = \mathrm{Re}\left[\int_{-\infty}^{\infty} dT_1 \int_{-\infty}^{\infty} dT_3 \times e^{i\omega_1 T_1 + i\omega_3 T_3}|R_{ech}(T_3,T_2,T_1)|\right]. \tag{22}$$

Here and hereafter, ω_1 and ω_3 are variables conjugate to the delay times T_1 and T_3, respectively (and are not the carrier frequencies of the first and third impulsive pulses).

In our simple case, we can show $S_{2D}(\omega_3,T_2,\omega_1)$ reduces to

$$S(\omega_1,\omega_3) = \sqrt{\frac{\pi}{2}}\,\frac{1}{2\Gamma_I} \times \mathrm{Re}\left[\frac{i}{\omega_+ + i\Gamma_H}\left\{F(\overline{\Omega}_+) + F(\overline{\Omega}_-)\right\}\right] \tag{23}$$

where

$$\overline{\Omega}_\pm = \frac{\omega_+ + i\Gamma_H \pm \omega_-/2}{\sqrt{2}\,\Gamma_I}. \tag{24}$$

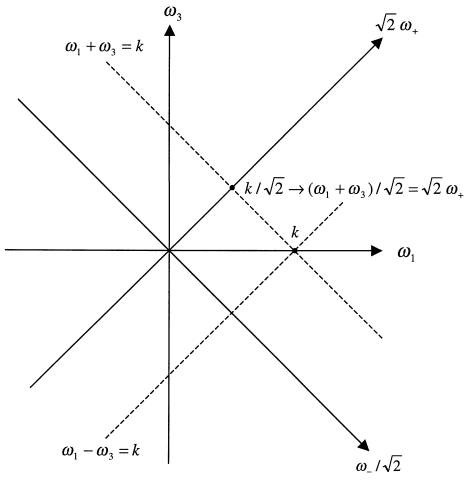

Fig. 2. The relation between (ω_1,ω_3) axes and (ω_+,ω_-) axes.

Here, $F(z)$ is the scaled complemented error function defined by $F(z)=\mathrm{e}^{-z^2}[1-\Phi(-iz)]$, where the error function is given by $\Phi(z)=2\int_0^z \mathrm{d}t\,\mathrm{e}^{-t^2}/\sqrt{\pi}$, and

$$\omega_-=\omega_1-\omega_3\,, \tag{25}$$

$$\omega_+=(\omega_1+\omega_3)/2\,. \tag{26}$$

The value of ω_+ increases along the diagonal direction on the $\omega_1-\omega_3$ plane, while the value of ω_- increases along the diagonal direction; ω_+ and ω_- axes are the diagonal and anti-diagonal axes, respectively. Note here the scale factors $\sqrt{2}$ and $1/\sqrt{2}$ for the diagonal and anti-diagonal axes, respectively (see Fig. 2).

Eq. (23) is an important result of our Letter. To shed light on the essential features, we consider the two limiting case as follows.

1. **Large (inhomogeneous) Gaussian broadening limit.** If $\Gamma_\mathrm{H}\ll\Gamma_\mathrm{I}$, the Lorentzian factor in Eq. (23) shows a peak sharp enough to let $\omega_+ + i\Gamma_\mathrm{H}=0$ in the remaining factors of $S(\omega_1,\omega_3)$. Noting the relation, $\Phi(-z)=-\Phi(z)$, we have

$$S(\omega_1,\omega_3)=\sqrt{\frac{\pi}{2}}\,\frac{1}{\Gamma_\mathrm{I}}\,\frac{\Gamma_\mathrm{H}}{\omega_+^2+\Gamma_\mathrm{H}^2}\,\mathrm{e}^{-\omega_-^2/(8\Gamma_\mathrm{I}^2)}\,. \tag{27}$$

Unlike the conventional 1DLS analysis, $S(\omega_1,\omega_3)$ is a simple product of the Lorentzian and Gaussian *with two independent frequency variables*. Thus, the diagonal and anti-diagonal widths directly give the Lorentzian and Gaussian widths, respectively (see Fig. 2). The introduction of two frequency variables allows us to separate the two contributions as oppose to the conventional 1DLS analysis.

2. **Small (inhomogeneous) Gaussian broadening limit.** When there is no inhomogeneity, from Eqs. (21) and (22), we have

$$S(\omega_1,\omega_3)=\frac{\Gamma_\mathrm{H}}{\omega_1^2+\Gamma_\mathrm{H}^2}\times\frac{\Gamma_\mathrm{H}}{\omega_3^2+\Gamma_\mathrm{H}^2}\,. \tag{28}$$

In this purely homogeneous limit, the 2DLS becomes symmetric in the homogeneous limit.

The original expression (23) is plotted in Fig. 3; the 11 contour lines are drawn where the maximum is scaled to the unity; only the positive contributions are explicitly displayed – the lowest contour line

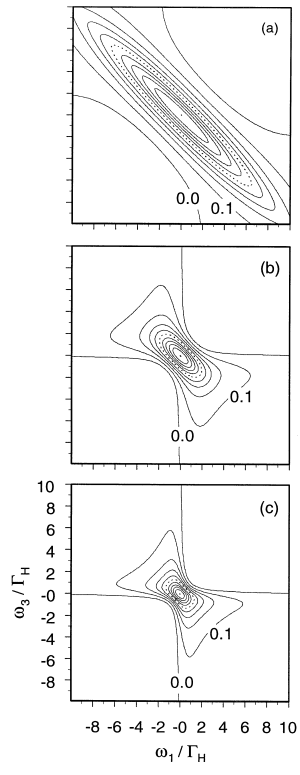

Fig. 3. The 2DLS calculated from Eq. (23). The dotted contour line corresponds to the half maximum. (a) $\Gamma_\mathrm{I}/\Gamma_\mathrm{H}=5$. (b) $\Gamma_\mathrm{I}/\Gamma_\mathrm{H}=1$. (c) $\Gamma_\mathrm{I}/\Gamma_\mathrm{H}=1/5$.

corresponding to zero. When the Gaussian width is fairly large compared with the Lorentzian width, as in Fig. 3a, we see that the 2D contour map looks elliptic and its major and minor axes at half maximum essentially give Γ_I and Γ_H, respectively, namely, the ellipticity directly corresponds to the ratio Γ_I/Γ_H. On the contrary, when the Gaussian width is small, as in Fig. 3c, we see that the contour map looks symmetric with respect to diagonal and off-diagonal axes. Considering also Fig. 3b, we conclude that the ellipticity of the 2D map is a clear indicator for the relative strength of the Gaussian width compared to the Lorentzian width; an elongated shape indicates a large 'inhomogeneity' while a symmetric shape corresponds to a 'homogeneous' line shape. Generally the diagonal and anti-diagonal slices through the 2DLS are related to the 'homogeneous' and 'inhomogeneous' broadening, respectively. On the contrary, the projection of the line shape on to the axis is a convolution of the Gaussian and Lorentzian contributions, and thus corresponds to the 1D absorption spectrum, as understood from Eq. (27) with setting $\omega_1 = 0$, or $\omega_3 = 0$.

As the indicator, the definition of the ellipticity has arbitrariness to some extent. Here, we define it as the ratio of the anti-diagonal width at the half maximum to the diagonal one. In the large Gaussian broadening limit represented by Eq. (27), the former is given by $2\omega_-/\sqrt{2} = 4\sqrt{\ln 2}\,\Gamma_I$, while the latter by $2\omega_+\sqrt{2} = 2\sqrt{2}\,\Gamma_H$ (note the scale factors $1/\sqrt{2}$ and $\sqrt{2}$ mentioned in the above); we see that the ratio is $1.2\,\Gamma_I/\Gamma_H$. In the opposite limit (Eq. (28)), the ratio is the unity. In other words, the ellipticity thus defined approaches to $1.2\,\Gamma_I/\Gamma_H$ and the unity as the ratio Γ_I/Γ_H gets large and small, respectively. In fact, the ellipticity for Fig. 3a,b,c are 7.5($=1.5\Gamma_I/\Gamma_H$), 2.8, and 2.1 where the ratio Γ_I/Γ_H are 5, 1, 1/5, respectively.

In this Letter, we have used two modes to represent two effective dynamical time scales, which are independent of one another. Solutions will more likely be characterized by a broad distribution of dynamical time scales, which would not lead to a clear time-scale separation. Our model is the simpler version, i.e., only two time scales which are independent and vary from fast to slow. The effects are clear in the 2DLS, and thereby this suggests that, in a more realistic model, similar effects will be observed. From these considerations, we can expect the present theory has the capability to describe the principle features even in the well-studied cases of complex chromophores in solution.

In conclusion, we propose to obtain the 2DLS by using the photon-echo signal with gated or heterodyne detection, and by 2D Fourier transformation of the absolute value of the signal with respect to the first and last delay times. The (homogeneous) Lorentzian and (inhomogeneous) Gaussian widths manifest themselves as the ellipticity of the 2DLS. The contours of the line shape can be used as a quantitative measure of the homogeneous and inhomogeneous widths. It is also the case that a quantitative analysis of the time-domain data will reveal the same level of quantitative information as the line-shape analysis, but only within the confines of this simple model. In a more complex system, composed of several lines or overtones, the spectral representation will be preferable over the oscillator nature of the time-domain version.

Acknowledgements

K.O. and Y.T. would like to thank Shaul Mukamel and David M. Jonas for sending stimulating papers [15,11]. A.T. acknowledges support from the National Science Foundation (CHE-9900342). The present work was supported by a Grant-in-Aid for Encouragement of Young Scientists and that for Scientific Research from the Japanese Ministry of Education, Science, Sports, and Culture.

References

[1] S. Mukamel, Principle of Nonlinear Optical Spectroscopy, Oxford, New York, 1995.
[2] L.R. Narasimhan, K.A. Littau, D.W. Pack, Y.S. Bai, A. Elschner, M.D. Fayer, Chem. Rev. 90 (1990) 439.
[3] A. Tokmakoff, M.D. Fayer, Acc. Chem. Res. 28 (1995) 437.
[4] M. Cho, G.R. Fleming, J. Phys. Chem. 98 (1994) 3478.
[5] H.C. Meijers, D.A. Wiersma, Phys. Rev. Lett. 68 (1992) 381.
[6] T. Joo, Y. Jia, J.-Y. Yu, M.J. Lang, G.R. Fleming, J. Chem. Phys. 104 (1996) 6089.
[7] W.P. de Boeij, M.S. Pshenichnikov, D.A. Wiersma, Chem. Phys. Lett. 253 (1996) 53.

[8] M.S. Pshenichnikov, K. Duppen, D.A. Wiersma, Phys. Rev. Lett. 74 (1995) 674.
[9] W.P. de Boeij, M.S. Pshenichnikov, D.A. Wiersma, Chem. Phys. Lett. 238 (1995) 1.
[10] M. Berg, D.A. Vanden Bout, Acc. Chem. Res. 30 (1997) 65.
[11] J.D. Hybl, A.W. Albrecht, S.M. Gallagher Faeder, D.M. Jonas, Chem. Phys. Lett. 297 (1998) 307.
[12] W.B. Bosma, Y.J. Yan, S. Mukamel, Phys. Rev. A 42 (1990) 6920.
[13] Y. Tanimura, K. Okumura, J. Chem. Phys. 106 (1997) 2078.
[14] R. Kubo, M. Toda, N. Hashitsume, Statistical Physics II, Springer, Berlin, 1995.
[15] S. Mukamel, A. Piryatinski, V. Chernyak, Acc. Chem. Res. 32 (1998) 145.